ACS OMEGA

Open Access

http://pubs.acs.org/journal/acsodf

Article

Utilization and Mechanisms of Tannic Acid as a Depressant for Chalcopyrite and Pyrite Separation

Da Sun, Maolin Li, Ming Zhang, Rui Cui, Zhiqiang Yang, Lingfeng Yu, Daowei Wang,* and Wei Yao*

Cite This: *ACS Omega* 2023, 8, 30474−30482

Read Online

ACCESS | Metrics & More | Article Recommendations

ABSTRACT: Current flotation practices using lime or cyanide as depressants in chalcopyrite and pyrite separation have significant disadvantages, such as substantial reagent consumption, high slurry pH, and environmental hazards. This work aimed to explore the utilization and mechanisms of tannic acid (TA) as an eco-friendly alternative to lime or cyanide in chalcopyrite−pyrite separation. Flotation results showed that TA selectively depressed pyrite yet allowed chalcopyrite to float at neutral or alkaline pH. Adsorption density and zeta potential results indicated that TA adsorbed intensely on pyrite but minorly on chalcopyrite. Besides, potassium ethyl xanthate was still largely adsorbed on chalcopyrite but not on pyrite after TA adsorption. Surface analysis by Fourier transform infrared spectroscopy and X-ray photoelectron spectroscopy further showed that the oxidation species of FeOOH and $Fe_2(SO_4)_3$, particularly FeOOH were the main active sites for TA chemical adsorption. Owing to the greater and faster oxidation of pyrite, more FeOOH and $Fe_2(SO_4)_3$ were generated on the pyrite surface, and the chemical adsorption of TA was more pronounced on the pyrite surface than on the chalcopyrite surface.

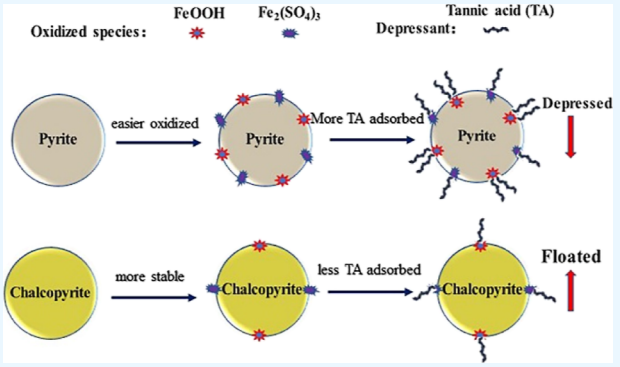

1. INTRODUCTION

Copper, an essential metal with diverse applications, has been serving as raw materials in many fields, including electricity, machinery, plumbing, chemistry, etc.[1,2] China has abundant copper resources; however, these copper ore deposits are characterized by low-grade, fine-grained, and complex mineralogy, typically coexisting with other minerals. Sulfide and oxide copper minerals are the two main copper-containing species that have been commercially exploited. As one of the vitally significant copper-bearing sulfide minerals, chalcopyrite ($CuFeS_2$) is the primary source of copper smelting.[3] In natural deposits, chalcopyrite often grows together with other sulfide minerals, particularly pyrite (FeS_2). In the beneficiation process of chalcopyrite, it is crucial to separate pyrite from chalcopyrite to obtain a high-grade copper concentrate.[4] Flotation is the dominant method for separating these two sulfide minerals. Both chalcopyrite and pyrite behave with good flotation permeability using thiol collectors in flotation. To enlarge the difference in surface hydrophilicity, cyanide and lime are two inorganic reagents that are commonly used to effectively depress pyrite yet allow chalcopyrite to float.[5] However, cyanide is well-known to be highly toxic and poses significant hazards to both human health and environmental safety.[6] Lime is generally considered to be nontoxic, but a large amount of it is needed to achieve an alkaline pulp pH as high as 12.0 for the effective depression of pyrite.[7] Consequently, this can lead to the accumulation of calcium ions in the pipeline, resulting in severe blockage.[8,9] Furthermore, lime addition causes sticky foam at high pH, which deteriorates the flotation process by increasing the mechanical entrainment of unwanted gangue minerals and therefore decreasing the quality of chalcopyrite concentrate.[10]

To address the aforementioned problems, organic depressants are increasingly being explored as promising alternatives to inorganic depressants in chalcopyrite−pyrite flotation separation. The structure of organic depressants, in particular the macromolecular organics, contains abundant hydrophilic groups (−OH, −COOH, etc.), some of which show chelating affinity capability toward mineral metal sites.[11] However, the weak solubility and limited selectivity of macromolecular organics attenuate their depression effects on gangue minerals and thus restrict their wide application.[12] Despite the excellent aqueous solubility of some small molecular organic depressants, their effectiveness is constrained by the smaller number of hydrophilic groups in the structure.[13] Therefore, a relatively high-molecular-weight depressant with plentiful hydrophilic

Received: May 25, 2023
Accepted: July 28, 2023
Published: August 11, 2023

https://doi.org/10.1021/acsomega.3c03663
ACS Omega 2023, 8, 30474−30482

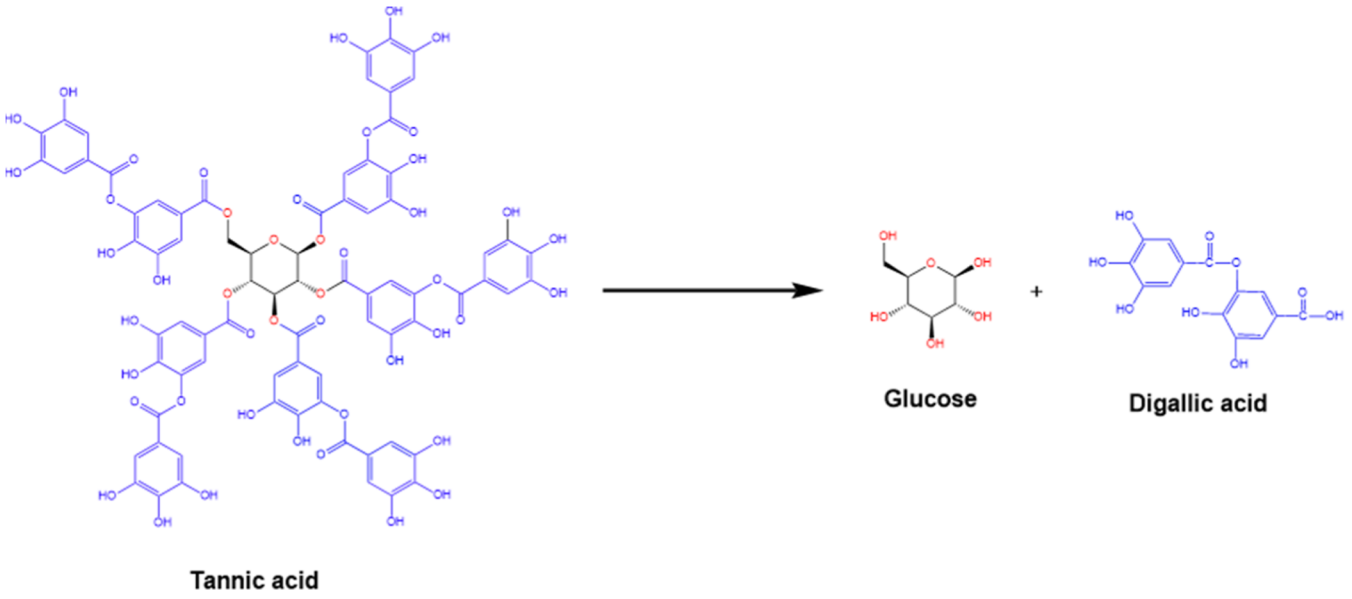

Figure 1. Chemical structure of TA and its hydrolysis products.

groups and high solubility holds promise as a green and effective depressant in chalcopyrite−pyrite separation.

Tannic acid (TA, $C_{76}H_{52}O_{46}$), a polyphenolic compound, is naturally extracted from plant tissues such as pods, cork oak, and sicilian lacquer leaves. The chemical formula of tannic is shown in Figure 1 with the basic structure of one glucose molecule bonded to as many as five digallic acid molecules.[14] It comprises numerous phenolic hydroxyls as the hydrophilic groups.[15] Additionally, as a weak acid, TA dissolves easily in water and hydrolyzes to generate hydrophilic glucose and digallic acid species. Owing to these natural characteristics, TA could be an effective organic depressant for flotation. Zhang et al. used TA in the separation of calcium-bearing minerals and found that TA selectively depressed calcite flotation from fluorite when TA was added before sodium oleate.[16] Besides, many literature studies also used tannins as depressants for iron-containing minerals including hematite, pyrite, marmatite, pyrrhotite, arsenopyrite, etc.[17−20] One important reason was a strong complexation interaction between metallic iron and tannins (Fe−TA) so that tannins can adsorb onto the surface of these minerals. However, the detailed adsorption process was not revealed clearly. In the case of pyrite flotation, pyrite is susceptible to oxidation in aqueous solution and can produce multiple oxidative species coating on pyrite surfaces. Depending on the oxidation degree and specific flotation conditions, the oxidation products may include iron oxides/hydroxides (FeO/FeOOH), sulfur/polysulfide (S_0/S_n^{2-}), and iron(II)/(III) sulfates.[21,22] It is not clear the target site through which TA can be anchored to pyrite surfaces. On the other hand, chalcopyrite processes better electrochemical stability in water compared to pyrite.[23] Since the existence of Fe in chalcopyrite crystals, it remains confusing regarding the selectivity of TA in chalcopyrite−pyrite flotation. In addition, many studies have demonstrated that proper oxidation of sulfide minerals would favor the adsorption and depression behavior of organic depressants.[24−27]

This work investigated the application of TA as a depressant in chalcopyrite−pyrite flotation using potassium ethyl xanthate as a collector. Microflotation was performed to examine the depression effectiveness of TA toward chalcopyrite and pyrite. The underlying mechanisms for the selective adsorption of TA were revealed by adsorption density tests, zeta potential measurements, Fourier transform infrared (FTIR) spectroscopy, and X-ray photoelectron spectroscopy (XPS).

2. EXPERIMENTAL SECTION

2.1. Materials. High-purity lump ores of chalcopyrite ($CuFeS_2$) and pyrite (FeS_2) were handpicked from the underground mine of Daye Iron Mine Co., Ltd., China. The −1.7 mm particles were ground by a laboratory ceramic mill. The grinding products were screened to obtain the −0.074 + 0.038 mm and −0.038 mm fractions, respectively. The −0.074 + 0.038 mm samples were utilized for microflotation experiments and XPS analysis. The −0.038 mm samples were used to conduct adsorption tests. Besides, a part of the −0.038 mm sample was ground finer (−0.005 mm) and utilized for zeta potential measurements and FTIR tests. The XRD spectra of chalcopyrite and pyrite are displayed in Figure 2, which indicates the high crystallinity with high purities of minerals. Additionally, the Cu and Fe grades of chalcopyrite and pyrite were 33.05 and 45.41%, respectively, indicating a purity of 95.03% for chalcopyrite and 97.30% for pyrite.

TA and potassium ethyl xanthate (KEX) purchased from Macklin Inc., China, were used as the depressant and collector, respectively. NaOH and HCl were used as the pH modifiers. Terpineol oil obtained from the Daye beneficiation plant was used as the frother. Deionized (DI) water with a conductivity of less than 5 μs/cm was used.

2.2. Microflotation Experiments. The flotation was performed on an XFG flotation machine. For each flotation, 2.0 g of mineral was mixed with 35 mL of DI water and then the spindle was started to rotate at 1680 rpm. Afterward, the reagents including pH modifiers, TA (if needed), KEX, and terpineol oil (1.0 μL) were added sequentially and stirred for 2, 4, 3, and 1 min, respectively. After 6 min of scraping the blister, products of concentrates and tailings were collected to calculate the flotation recovery. The flotation flowsheet is shown in Figure 3.

2.3. Adsorption Density Tests. The KEX adsorption density on chalcopyrite and pyrite after TA adsorption was

https://doi.org/10.1021/acsomega.3c03663
ACS Omega 2023, 8, 30474−30482

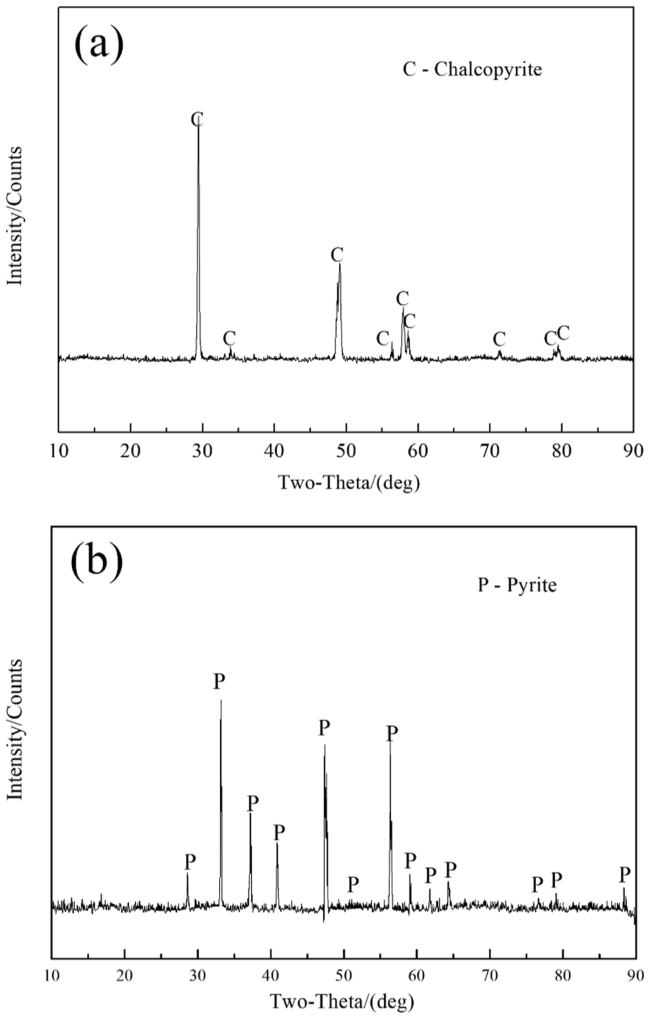

Figure 2. XRD spectra of (a) chalcopyrite and (b) pyrite.

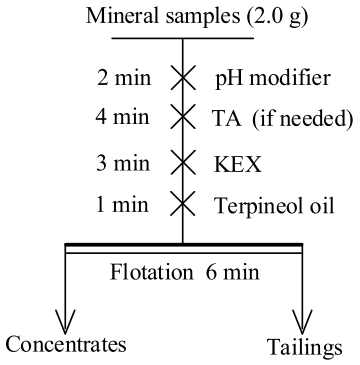

Figure 3. Flowsheet of microflotation experiments.

measured by using a UV2550 spectrophotometer. The prepared sample followed the microflotation process. After all the reagents were added and conditioned, the pulp was settled for 10 min and then the supernatant was centrifuged for at least 30 min. The supernatant of the centrifuged pulp was injected into a quartz cuvette for testing.

2.4. Zeta Potential Measurements. For preparation, 0.05 g of mineral samples (−0.005 mm) and 35 mL of KCl (1.0×10^{-3} mol/L) electrolyte water were mixed. Then, certain concentrations of reagents were dropped into the pulp and stirred following the procedure of microflotation. Subsequently, the pulp had 10 min settlement and the supernatant was taken out for testing.

2.5. FTIR Tests. The test samples were prepared by mixing 2.0 g of mineral (−0.005 mm) and 35 mL of DI water and then treated with TA which was in line with the flotation. After the interaction, the pulp was filtered, washed three times using DI water, and vacuum-dried below 50 °C. The dried sample was sent to test.

2.6. XPS Tests. In this research, the powder sample was prepared following the same process as FTIR tests. After preparation, the samples were sent to the laboratory for tests.

3. RESULTS AND DISCUSSION

3.1. Microflotation Experiments. Figure 4 depicts the flotation recoveries of chalcopyrite and pyrite at various TA concentrations (a) and pulp pH values (b). As depicted in Figure 4a, both chalcopyrite and pyrite exhibited good flotation by KEX with an approximate recovery of 94.0% without TA treatment. As the TA concentration increased to 10 mg/L, a subtle decrease (about 5%) in chalcopyrite recovery was observed, indicating that TA had a minor deteriorating effect on chalcopyrite flotation within the experimental concentrations. In the case of pyrite flotation, when the TA concentration increased from zero to 1.25 mg/L,

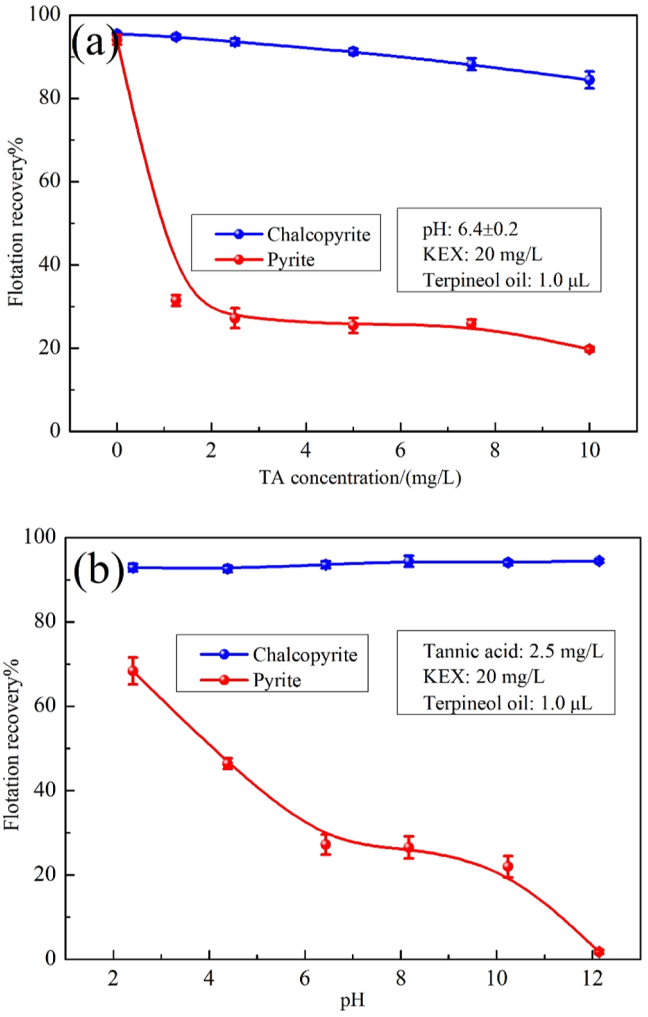

Figure 4. Flotation recoveries of chalcopyrite and pyrite at various (a) TA concentrations and (b) pH values.

https://doi.org/10.1021/acsomega.3c03663
ACS Omega 2023, 8, 30474−30482

the pyrite recovery decreased quickly from 94.0 to 31.5%, suggesting that TA had a strong inhibition on pyrite. Sequentially, with further growth in TA concentration (1.25−7.5 mg/L), the flotation recovery of pyrite remained as low as 26.0%. Furthermore, the pyrite flotation recovery had a further slight decrease with the TA concentration increasing to 10 mg/L, indicating that a higher TA concentration resulted in a stronger depression effect. By comparison of the flotation recovery gaps of the two curves shown in Figure 4a, it can be concluded that the optimal concentration of TA was 2.5 mg/L.

Figure 4b shows the flotation recoveries of chalcopyrite and pyrite at various pH values. For the chalcopyrite flotation, the recovery remained at around 93.0% regardless of the slurry pH. It suggests that TA had a minor impact on chalcopyrite floatability over the pH range of 2−12. On the other hand, the depression of pyrite by TA was dependent on pulp pH. In acidic conditions (pH < 5), the depression was relatively weak and pyrite recovery was still above 40%. While the pyrite recovery decreased apparently with increasing pH, it was strongly depressed in the high alkaline pulp. The more pronounced depression effect at higher pH was likely caused by the faster and stronger oxidation of pyrite, which generated more hydrophilic FeOOH and $Fe_2(SO_4)_3$ species on its surface.[28] By contrast, the oxidation products would be dissolved at acidic pH particularly when pulp pH was as low as 2.4, which may decrease the adsorption sites of TA.[29]

3.2. Adsorption Density Tests. Figure 5 presents the adsorption density of KEX on the mineral surfaces at different

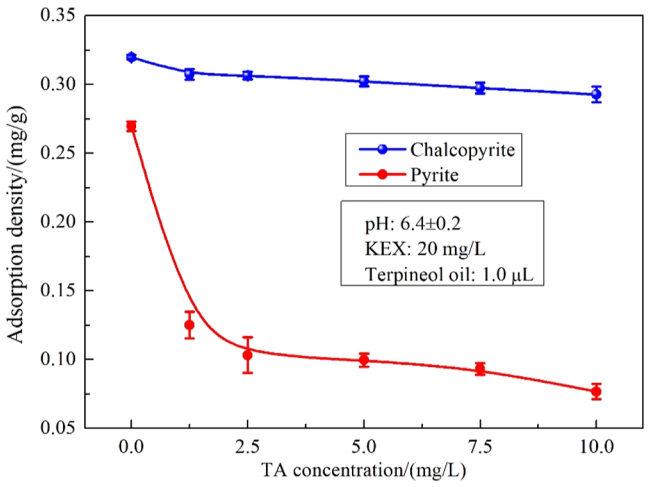

Figure 5. Adsorption density of KEX on chalcopyrite and pyrite surfaces at various TA concentrations.

TA concentrations. As depicted, the KEX on chalcopyrite was kept at a high level with increasing TA concentration to 10 mg/L. It indicates that TA could barely adsorb on the chalcopyrite surface and had negligible effects on KEX adsorption, which explained the high recovery of chalcopyrite in microflotation tests. For the KEX adsorption on the pyrite surface, when TA was added and increased to 1.25 mg/L, the adsorption capacity decreased sharply, indicating that TA strongly prevented KEX from adsorbing on the pyrite surface. With further increasing the TA concentration, the adsorption capacity decreased slowly, the trend of which agreed well with flotation results. Obviously, the KEX density on chalcopyrite was much denser than that on pyrite, thus a high flotation recovery of chalcopyrite. While TA could adsorb strongly and occupy the target sites on pyrite, thus the subsequent KEX adsorption was hindered.

3.3. Zeta Potential Measurements. As illustrated in Figure 6a, the zeta potential of chalcopyrite decreased as the

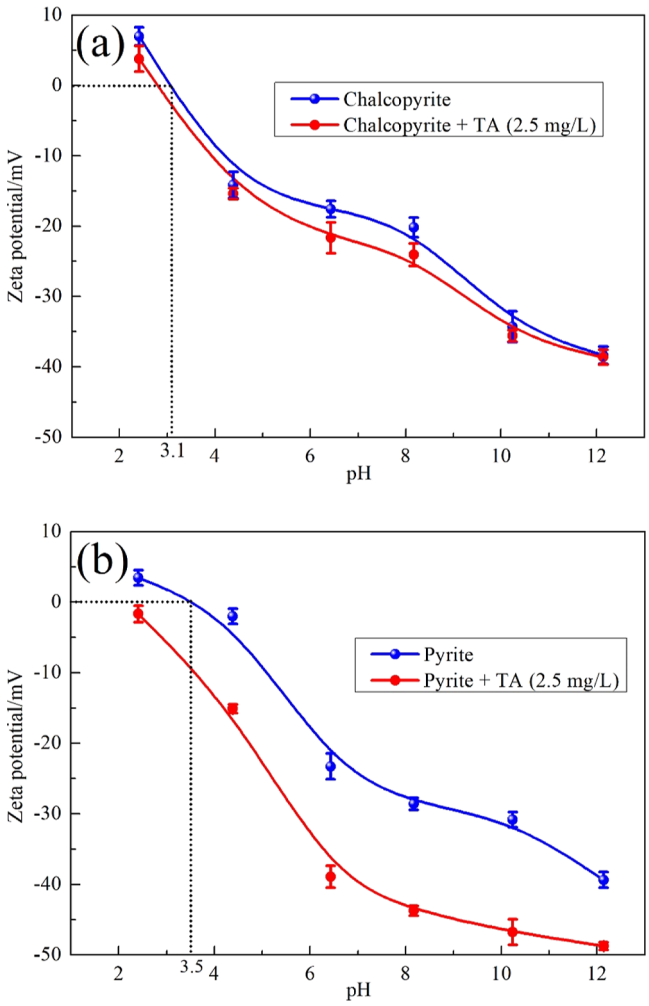

Figure 6. Zeta potentials of (a) chalcopyrite and (b) pyrite before and after treatment with TA at various pH values.

pH increased. Additionally, the isoelectric point was located at pH = 3.1 which was along with the published papers.[30,31] After the addition of TA, the zeta potential of chalcopyrite shifted negatively, suggesting the adsorption of TA ions.[32] However, the negative shift was minor (less than 4 mV), implying that TA was weakly adsorbed on chalcopyrite.

Figure 6b illustrates the zeta potential of pyrite with and without TA. Without TA, the curve of pyrite was similar to that of chalcopyrite, and the isoelectric point was located at 3.5 which was in the same range as the reported results in the literature.[33,34] When the pyrite was treated by TA, the zeta potential had a larger decrease (as high as 16 mV) compared to TA-treated chalcopyrite. This implied that TA possessed stronger adsorption toward pyrite than chalcopyrite.[32] Moreover, the decreased values at acidic pH were lower than those at natural and alkaline pH, indicating that TA adsorption was less pronounced at acidic pH and had a weak affinity with pyrite.[35] This may result from the dissolution of oxidized products at strong acidic pH which eliminated the adsorption sites of TA.[29]

https://doi.org/10.1021/acsomega.3c03663
ACS Omega 2023, 8, 30474−30482

3.4. FTIR Analysis. As depicted in Figure 7a, the TA curve exhibited a broad band at 3382.19 cm^{-1}, which was assigned to

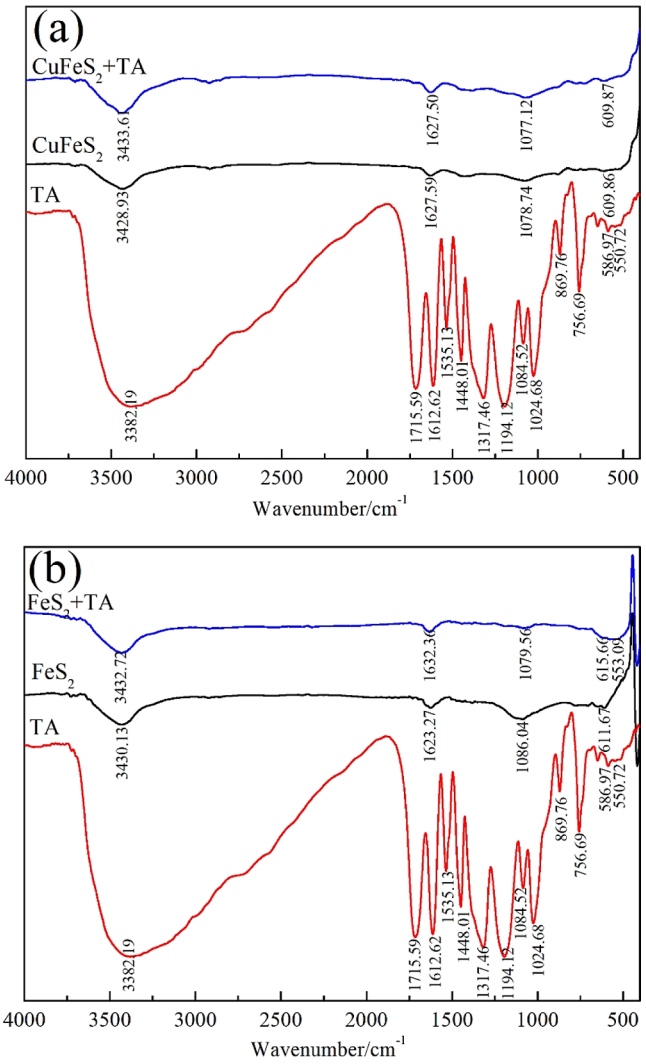

Figure 7. FTIR spectra of (a) chalcopyrite and (b) pyrite before and after treatment with TA.

the phenolic hydroxyl.[36] The 1715.59 and 1317.46 cm^{-1} values were associated with the carboxyl carbonyl group and phenol group, respectively. The 1612.62 and 1535.13 cm^{-1} were induced by the −C═C− aromatic ring.[20] The 1448.01 and 1194.12 cm^{-1} were owned by the aromatic C−C and stretching vibrations of C−O, respectively.[37] Additionally, the 1100−1000 cm^{-1} range accounted for C−O and C−H deformations, and another range of 900−550 cm^{-1} belonged to the C−H bonds of the benzene ring.[38] In the chalcopyrite spectrum, 3428.93 cm^{-1} was assigned to the vibration of liquid water which originated from the atmosphere during testing. Importantly, the weak 1078.74 and 609.86 cm^{-1} were ascribed to SO_4^{2-},[39,40] indicating slight oxidation of chalcopyrite.[41] When TA was added, the bands of liquid water and SO_4^{2-} still existed with shifts lower than 2.00 cm^{-1}. This implied that TA weakly interacted with chalcopyrite, which was consistent with zeta potential results.

In the spectrum of pure pyrite, the band of liquid water appeared at 3430.13 cm^{-1}, and the two bands of SO_4^{2-} appeared at 1086.04 and 611.67 cm^{-1}. Notably, the band areas of SO_4^{2-} were larger for pyrite than for chalcopyrite, indicating deeper and stronger oxidation on the pyrite surface. Upon treatment with TA, the bands of SO_4^{2-} shifted as much as 7.00 cm^{-1}, suggesting stronger chemical adsorption of TA on pyrite. However, the band areas were smaller than those observed before treatment, which may be attributed to the interaction between oxidation products and TA. Furthermore, the band at 1623.27 cm^{-1} on the pyrite surface after treatment with TA shifted by 9 cm^{-1} compared to that before treatment with TA, likely due to the −C═C− aromatic ring of the adsorbed TA on pyrite. Additionally, 553.09 cm^{-1} appeared as a new band that may contribute to the C−H bonds of the benzene ring. These further implied the stronger chemical adsorption of TA on pyrite.

3.5. XPS Analysis. As presented in Figure 8a, the Cu 2p, Fe 2p, O 1s, C 1s, and S 2p peaks were detected in the spectra

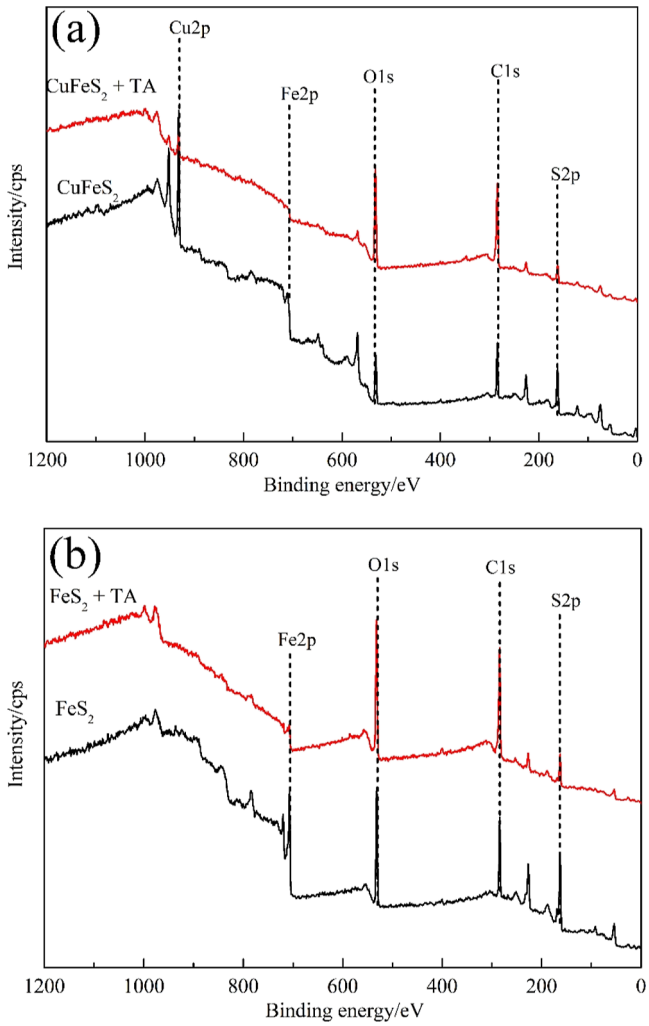

Figure 8. XPS survey spectrum of (a) chalcopyrite and (b) pyrite before and after treatment with TA.

of chalcopyrite both with and without TA treatment. Cu, Fe, and S were the constituent elements of chalcopyrite while C was the background for the XPS test.[42] The presence of O may originate from the testing environment and the oxidation of chalcopyrite.[43] To the atomic contents shown in Table 1, for chalcopyrite, the C and O contents were 39.88 and 17.13%, respectively, for the bare chalcopyrite sample. After interaction

https://doi.org/10.1021/acsomega.3c03663
ACS Omega 2023, 8, 30474−30482

Table 1. Atomic Contents on Chalcopyrite and Pyrite Surfaces before and after Treatment with TA

sample	atomic contents/%				
	S 2p	C 1s	O 1s	Fe 2p	Cu 2p
chalcopyrite	21.9	39.88	17.13	8.58	12.51
chalcopyrite + TA	17.57	50.73	19.96	3.72	8.02
pyrite	21.35	42.57	27.29	8.79	
pyrite + TA	6.26	57.42	31.16	5.16	

with TA, C and O contents increased to 50.73 and 19.96%, respectively, suggesting that TA was adsorbed on chalcopyrite. In the case of pyrite, Fe 2p, O 1s, C 1s, and S 2p were detected in the two spectra. The contents of C and O were 42.57 and 27.29%, respectively, on the surface of bare pyrite. It was noted that the O content was much higher than that on the chalcopyrite surface, suggesting a more pronounced and stronger oxidation degree of the pyrite surface. After TA addition, the C and O contents were increased by 14.85 and 3.87%, respectively, which were much larger than those on the chalcopyrite surface, particularly for the C content. This indicated that TA adsorbed strongly with a higher adsorption density on the pyrite surface.

To confirm the target sites between TA and chalcopyrite and pyrite surfaces, the XPS narrow spectra with fitting peaks were analyzed (Figures 9 and 10). Figure 9 shows the high-resolution spectrum of Fe $2p_{3/2}$. Before treatment with TA, three peaks presented on the pure chalcopyrite at 707.58, 709.76, and 712.06 eV, which were assigned to the Fe $2p_{3/2}$ in $CuFeS_2$, FeOOH, and $Fe_2(SO_4)_3$, respectively.[44] FeOOH and $Fe_2(SO_4)_3$ were the oxidation species of chalcopyrite.[45] After treatment with TA, the three peaks changed to 707.67, 709.90, and 712.20 eV, respectively, with minor shifts (lower than 0.15 eV) compared with those on pure chalcopyrite surface, indicating the weak affinity and limited chemical adsorption of TA on chalcopyrite. For pyrite shown in Figure 9b, the binding energies of 707.40, 709.28, and 711.93 eV were detected and identified as FeS_2, FeOOH, and $Fe_2(SO_4)_3$, respectively. After treatment with TA, they shifted to 707.41, 710.08, and 712.32 eV with 0.01, 0.80, and 0.39 eV changes, respectively. By comparison, it implied that TA was intensely and chemically adsorbed on pyrite, and it mainly interacted with the surface oxidation products, particularly FeOOH.

Figure 10 shows the O 1s on chalcopyrite and pyrite before and after treatment with TA. Before treatment, as depicted in Figure 10a, the 530.33 and 531.75 eV peaks were ascribed to H_2O and O_2, respectively, which may be adsorbed from the air during testing.[46,47] The peak at 533.15 eV was attributed to OOH/SO_4^{2-}, which originated from the oxidation of chalcopyrite.[4] When TA interacted with chalcopyrite, the peaks of H_2O, O_2, and OOH/SO_4^{2-} appeared at 530.47, 533.70, and 533.05 eV, respectively. The shifts of those three peaks were minor (lower than 0.15 eV), indicating the weak adsorption of TA on chalcopyrite. In addition, 533.70 eV was detected as a new peak, resulting from the C═O bond in TA. This also indicated the adsorption of TA. In the case of pyrite, the peaks of H_2O, O_2, and OOH/SO_4^{2-} were detected at 530.38, 531.90, and 533.10 eV, respectively. After treatment with TA, the H_2O and O_2 peaks shifted slightly to 530.37 and 531.82 eV, respectively. However, the peak of the OOH/SO_4^{2-} ion shifted significantly to 532.73 eV, indicating the strong chemical adsorption of TA on pyrite. Furthermore, a large C═O peak originating from TA was shown, further suggesting the strong chemical adsorption of TA on pyrite.

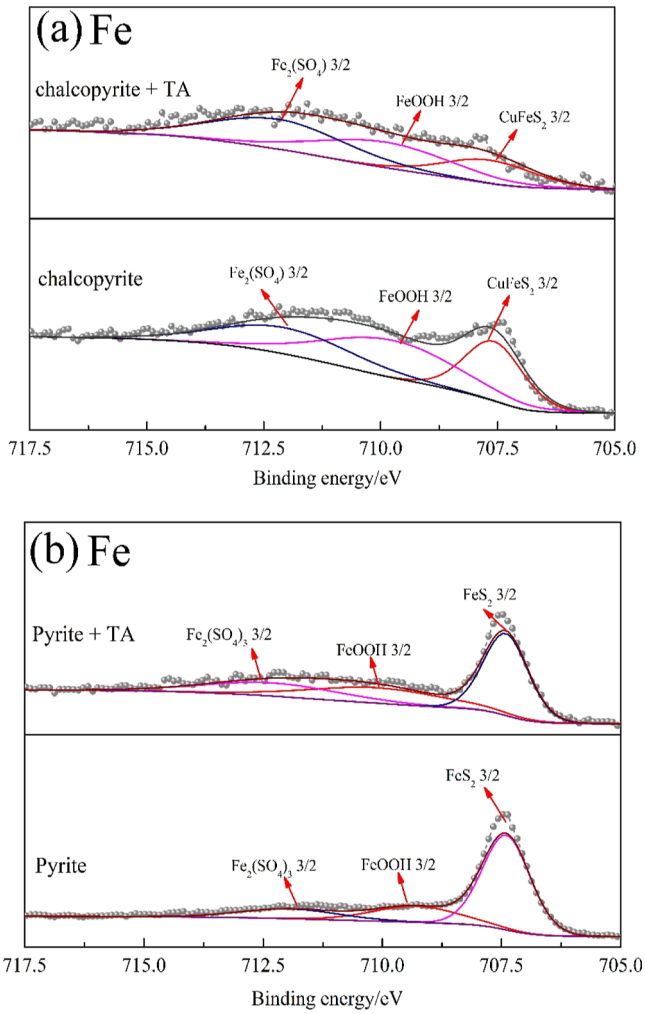

Figure 9. XPS narrow spectrum of Fe on (a) chalcopyrite and (b) pyrite before and after treatment with TA.

According to the above results and analysis, it could be drawn that TA was a selective depressant in chalcopyrite−pyrite flotation. TA was largely adsorbed on the pyrite surface chemically and impeded the subsequent KEX adsorption, while the results were contrary on the chalcopyrite surface. The surface oxidation differences on chalcopyrite and pyrite resulted in different adsorption of TA and subsequent KEX on mineral surfaces and thus the different flotation behavior of chalcopyrite and pyrite. Pyrite was readily oxidized in the flotation process and generated a higher density of FeOOH and $Fe_2(SO_4)_3$ species compared to chalcopyrite. These oxidizing species served as active adsorption sites for TA molecules, resulting in a higher chemical adsorption density on pyrite.

4. CONCLUSIONS

In this research, TA was used as an eco-friendly depressant in chalcopyrite−pyrite separation. The flotation behavior of chalcopyrite and pyrite under TA depressant was investigated by microflotation experiments, and the adsorption density tests, zeta potential measurements, FTIR analysis, and XPS tests were conducted to reveal the mechanisms. The results showed that TA (2.5 mg/L) had a negligible effect on

https://doi.org/10.1021/acsomega.3c03663
ACS Omega 2023, 8, 30474−30482

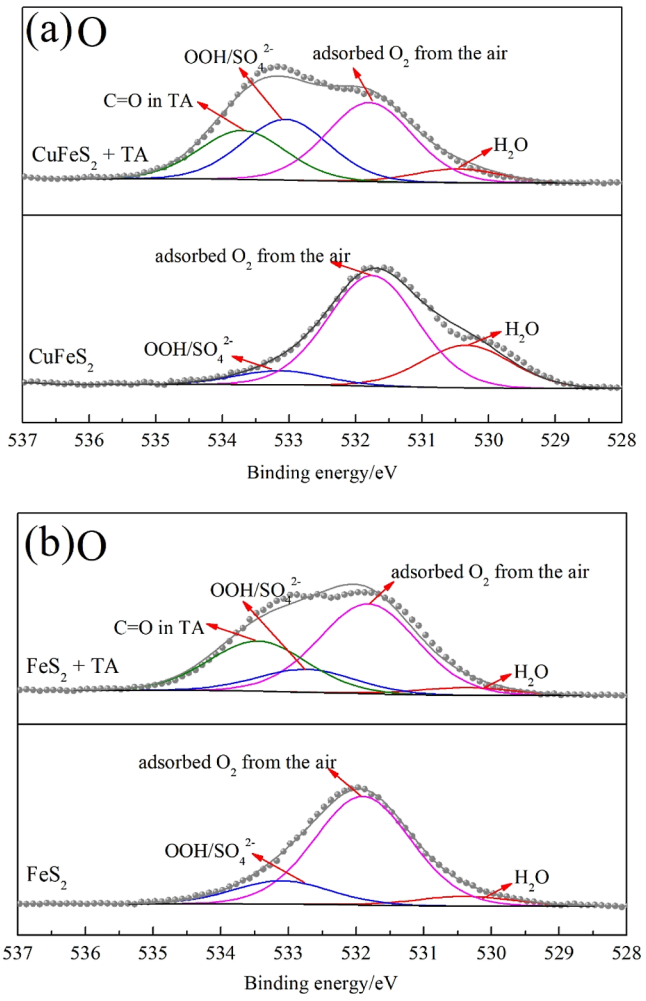

Figure 10. XPS narrow spectrum of O 1s on (a) chalcopyrite and (b) pyrite before and after treatment with TA.

chalcopyrite flotation but strongly depressed pyrite under a neutral or alkaline pH. TA was intensely chemically adsorbed on pyrite and blocked the subsequent adsorption of KEX. In contrast, weak adsorption of TA was found on chalcopyrite, and KEX could still function effectively and float chalcopyrite. The oxidation species of $Fe_2(SO_4)_3$ and particularly FeOOH on the chalcopyrite and pyrite surfaces served as the chemical adsorption sites for TA, but the chemical adsorption was more significant on pyrite owing to its stronger oxidation and higher density of FeOOH and $Fe_2(SO_4)_3$ species on the surface.

AUTHOR INFORMATION

Corresponding Authors

Daowei Wang − *Department of Chemical and Materials Engineering, University of Alberta, Edmonton, Alberta T6G 1H9, Canada*; Email: daowei@ualberta.ca

Wei Yao − *School of Resources and Environmental Engineering, Wuhan University of Science and Technology, Wuhan 430081, People's Republic of China; Hubei Key Laboratory for Efficient Utilization and Agglomeration of Metallurgic Mineral Resources, Wuhan 430081, People's Republic of China*; orcid.org/0000-0002-7864-1137; Email: yaowei1990520@163.com

Authors

Da Sun − *School of Resources and Environmental Engineering, Wuhan University of Science and Technology, Wuhan 430081, People's Republic of China; Hubei Key Laboratory for Efficient Utilization and Agglomeration of Metallurgic Mineral Resources, Wuhan 430081, People's Republic of China; Wuhan Kaisheng Technology Co., Ltd., Wuhan 430070, People's Republic of China*

Maolin Li − *School of Resources and Environmental Engineering, Wuhan University of Science and Technology, Wuhan 430081, People's Republic of China; Hubei Key Laboratory for Efficient Utilization and Agglomeration of Metallurgic Mineral Resources, Wuhan 430081, People's Republic of China; Changsha Research Institute of Mining and Metallurgy Co., Ltd., Changsha 410012, People's Republic of China*

Ming Zhang − *School of Resources and Environmental Engineering, Wuhan University of Science and Technology, Wuhan 430081, People's Republic of China; Hubei Key Laboratory for Efficient Utilization and Agglomeration of Metallurgic Mineral Resources, Wuhan 430081, People's Republic of China*; orcid.org/0000-0001-9415-4198

Rui Cui − *School of Resources and Environmental Engineering, Wuhan University of Science and Technology, Wuhan 430081, People's Republic of China; Hubei Key Laboratory for Efficient Utilization and Agglomeration of Metallurgic Mineral Resources, Wuhan 430081, People's Republic of China*

Zhiqiang Yang − *School of Resources and Environmental Engineering, Wuhan University of Science and Technology, Wuhan 430081, People's Republic of China*

Lingfeng Yu − *School of Resources and Environmental Engineering, Wuhan University of Science and Technology, Wuhan 430081, People's Republic of China*

Complete contact information is available at: https://pubs.acs.org/10.1021/acsomega.3c03663

Author Contributions

Da Sun: conceptualization, methodology, investigation, data curation, and writing—original draft. **Maolin Li**: conceptualization and methodology. **Ming Zhang**: writing—review and editing. **Rui Cui, Zhiqiang Yang, and Lingfeng Yu**: resources and formal analysis. **Daowei Wang**: conceptualization, methodology, and writing—review and editing. **Wei Yao**: conceptualization, methodology, data curation, formal analysis, writing—original draft, and writing—review and editing.

Notes

The authors declare no competing financial interest.

ACKNOWLEDGMENTS

The authors would like to thank the National Natural Science Foundation of China (Project no. 51704214 and 51704215) and "the 14th Five Year Plan" Hubei Provincial advantaged characteristic disciplines (groups) project of Wuhan University of Science and Technology (2023A0401) for support. The authors would also thank the Shiyanjia Lab (https://www.shiyanjia.com/) for the XRD, FTIR, and XPS tests.

REFERENCES

(1) Huang, Z.; Wang, J.; Sun, W.; Hu, Y.; Cao, J.; Gao, Z. Selective flotation of chalcopyrite from pyrite using diphosphonic acid as collector. *Miner. Eng.* **2019**, *140*, 105890.

(2) Zhang, X.; Xiong, W.; Lu, L.; Qian, Z.; Zhu, Y.; Mkhonto, P. P.; Zheng, Y.; Han, L.; Ngoepe, P. E. A novel synthetic polymer depressant for the flotation separation of chalcopyrite and galena and insights into its interfacial adsorption mechanism. *Sep. Purif. Technol.* **2021**, *279*, 119658.
(3) Wang, C.; Liu, R.; Wu, M.; Zhai, Q.; Luo, Y.; Jing, N.; Xie, F.; Sun, W. Selective separation of chalcopyrite from sphalerite with a novel depressant fenugreek gum: Flotation and adsorption mechanism. *Miner. Eng.* **2022**, *184*, 107653.
(4) Yang, X.; Li, Y.; Fan, R.; Duan, W.; Huang, L.; Xiao, Q. Separation mechanism of chalcopyrite and pyrite due to H_2O_2 treatment in low-alkaline seawater flotation system. *Miner. Eng.* **2022**, *176*, 107356.
(5) Han, G.; Wen, S.; Wang, H.; Feng, Q.; Bai, X. Pyrogallic acid as depressant for flotation separation of pyrite from chalcopyrite under low-alkalinity conditions. *Sep. Purif. Technol.* **2021**, *267*, 118670.
(6) Shen, Z.; Wen, S.; Han, G.; Zhou, Y.; Bai, X.; Feng, Q. Selective depression mechanism of locust bean gum in the flotation separation of chalcopyrite from pyrite in a low-alkalinity media. *Miner. Eng.* **2021**, *170*, 107044.
(7) Khoso, S. A.; Hu, Y.; Tian, M.; Gao, Z.; Sun, W. Evaluation of green synthetic depressants for sulfide flotation: Synthesis, characterization and floatation performance to pyrite and chalcopyrite. *Sep. Purif. Technol.* **2021**, *259*, 118138.
(8) Qin, X.; Liu, J.; Yu, Y.; Hao, J.; Gao, H.; Li, D.; Dai, L. Novel application of depressant sodium mercaptoacetate in flotation separation of chalcopyrite and pyrite. *Adv. Powder Technol.* **2023**, *34* (9), 104141.
(9) Sun, X.; Huang, L.; Wu, D.; Tong, X.; Yang, S.; Hu, B. The selective depression effect of dextrin on pyrite during the Zn-Fe sulfides flotation under low alkaline conditions. *Colloids Surf., A* **2022**, *650*, 129573.
(10) Tang, Y.; Wang, T.; Hu, Z. Research progress of flotation agents for Cu-S separation flotation. *Mater. Res. Appl.* **2012**, *6* (2), 100−103.
(11) Liu, C.; Zhou, M.; Xia, L.; Fu, W.; Zhou, W.; Yang, S. The utilization of citric acid as a depressant for the flotation separation of Barite from fluorite. *Miner. Eng.* **2020**, *156*, 106491.
(12) Dong, L.; Jiao, F.; Qin, W.; Liu, W. Selective flotation of scheelite from calcite using xanthan gum as depressant. *Miner. Eng.* **2019**, *138*, 14−23.
(13) Dong, L.; Wei, Q.; Qin, W.; Jiao, F. Effect of iron ions as assistant depressant of citric acid on the flotation separation of scheelite from calcite. *Chem. Eng. Sci.* **2021**, *241*, 116720.
(14) Hem, J. D. *Complexes of Ferrous Iron with Tannic Acid*; United States Government Printing Office: WA, 1960; pp 77−79.
(15) Wang, D.; Wang, D.; Deng, C.; Wang, K.; Tan, X.; Liu, Q. Flocculation of quartz by a dual polymer system containing tannic acid and poly(ethylene oxide): Effect of polymer chemistry and hydrodynamic conditions. *Chem. Eng. J.* **2022**, *446*, 137403.
(16) Zhang, C.; Wei, S.; Hu, Y.; Tang, H.; Gao, J.; Yin, Z.; Guan, Q. Selective adsorption of tannic acid on calcite and implications for separation of fluorite minerals. *J. Colloid Interface Sci.* **2018**, *512*, 55−63.
(17) Fraga-Corral, M.; García-Oliveira, P.; Pereira, A. G.; Lourenço-Lopes, C.; Jimenez-Lopez, C.; Prieto, M. A.; Simal-Gandara, J. Technological application of tannin-based extracts. *Molecules* **2020**, *25*, 614.
(18) Tohry, A.; Dehghan, R.; de Salles Leal Filho, L.; Chehreh Chelgani, S. Tannin: An eco-friendly depressant for the green flotation separation of hematite from quartz. *Miner. Eng.* **2021**, *168*, 106917.
(19) Asimi Neisiani, A.; Saneie, R.; Mohammadzadeh, A.; Wonyen, D. G.; Chehreh Chelgani, S. Biodegradable hematite depressants for green flotation separation-An overview. *Miner. Eng.* **2023**, *199*, 108114.
(20) Han, G.; Wen, S.; Wang, H.; Feng, Q. Interaction mechanism of tannic acid with pyrite surfaces and its response to flotation separation of chalcopyrite from pyrite in a low-alkaline medium. *J. Mater. Res. Technol.* **2020**, *9* (3), 4421−4430.
(21) Zhang, W.; Jiang, X.; Ralston, J.; Cao, J.; Jin, X.; Sun, W.; Gao, Z. Efficient heterogeneous photodegradation of Eosin Y by oxidized pyrite using the photo-Fenton process. *Miner. Eng.* **2023**, *191*, 107972.
(22) Hu, J.; Zhou, S.; Liao, S.; Gu, G.; Wang, Y. Effect of oxidized pyrite activating persulfate on the degradation of aniline aerofloat: Mechanism and degradation pathway. *Miner. Eng.* **2023**, *201*, 108233.
(23) Wu, J.; Ma, W.; Wang, X.; Jiao, F.; Qin, W. The effect of galvanic interaction between chalcopyrite and pyrite on the surface chemistry and collector adsorption: Flotation and DFT study. *Colloids Surf., A* **2020**, *607*, 125377.
(24) Jiao, F.; Cui, Y.; Wang, D.; Hu, C. Research of the replacement of dichromate with depressants mixture in the separation of copper-lead sulfides by flotation. *Sep. Purif. Technol.* **2021**, *278*, 119330.
(25) Jiang, K.; Liu, J.; Wang, Y.; Zhang, D.; Han, Y. Surface properties and flotation inhibition mechanism of air oxidation on pyrite and arsenopyrite. *Appl. Surf. Sci.* **2023**, *610*, 155476.
(26) Feng, B.; Zhong, C.; Zhang, L.; Guo, Y.; Wang, T.; Huang, Z. Effect of surface oxidation on the depression of sphalerite by locust bean gum. *Miner. Eng.* **2020**, *146*, 106142.
(27) Feng, B.; Jiao, X.; Wang, H.; Peng, J.; Yang, G. Improving the separation of chalcopyrite and galena by surface oxidation using hydroxyethyl cellulose as depressant. *Miner. Eng.* **2021**, *160*, 106657.
(28) Feng, Q.; Chen, J. *Electrochemistry of sulfide minerals flotation*; Central South University Press: Changsha, 2014; pp 30−34.
(29) Wang, D.; Hu, Y. *Solution chemistry of flotation*; Hunan Science and Technology Press: Changsha, 1987; pp 180−188.
(30) Wu, S.; Wang, J.; Tao, L.; Fan, R.; Wang, C.; Sun, W.; Gao, Z. Selective separation of chalcopyrite from pyrite using an acetylacetone-based lime-free process. *Miner. Eng.* **2022**, *182*, 107584.
(31) Sun, W.; Dai, S.; Zhang, H.; Chen, Y.; Yu, X.; Li, P.; Liu, W. Selective flotation of chalcopyrite from galena using a novel collector benzoic diethylcarbamothioic thioanhydride: An experimental and theoretical investigation. *J. Mol. Liq.* **2022**, *365*, 120027.
(32) Yao, W.; Li, M.; Zhang, M.; Cui, R.; Jiang, H.; Li, Y.; Zhou, S. Effects of grinding media on flotation performance of calcite. *Miner. Eng.* **2019**, *132*, 92−94.
(33) Chen, Y.; Zhang, G.; Shi, Q.; Yang, S.; Liu, D. Utilization of tetrasodium iminodisuccinate to eliminate the adverse effect of serpentine on the flotation of pyrite. *Miner. Eng.* **2020**, *150*, 106235.
(34) Forson, P.; Zanin, M.; Skinner, W.; Asamoah, R. Differential flotation of pyrite and arsenopyrite: Effect of hydrogen peroxide and collector type. *Miner. Eng.* **2021**, *163*, 106808.
(35) Liu, R.; Li, J.; Wang, Y.; Liu, D. Flotation separation of pyrite from arsenopyrite using sodium carbonate and sodium humate as depressants. *Colloids Surf., A* **2020**, *595*, 124669.
(36) Leonida, M. D.; Benzecry, A.; Lozanovska, B.; Mahmoud, Z.; Reid, A.; Belbekhouche, S. Impact of tannic acid on nisin encapsulation in chitosan particles. *Int. J. Biol. Macromol.* **2023**, *233*, 123489.
(37) Sethulekshmi, A. S.; Saritha, A.; Joseph, K.; Aprem, A. S.; Sisupal, S. B.; Sidharth, G.; Nair, V. S. Tannic acid as a green exfoliating agent: A sustainable pathway towards the development of natural rubber- molybdenum disulfide nanocomposites. *Ind. Crops Prod.* **2023**, *192*, 115978.
(38) Erdem, P.; Bursali, E. A.; Yurdakoc, M. Preparation and characterization of tannic acid resin: study of boron adsorption. *Environ. Prog. Sustainable Energy* **2013**, *32*, 1036−1044.
(39) Liu, D.; Zhang, G.; Chen, Y. Investigations on the selective depression of fenugreek gum towards galena and its role in chalcopyrite-galena flotation separation. *Miner. Eng.* **2021**, *166*, 106886.
(40) Weng, S. *Fourier transform infrared spectroscopy analysis*, 2nd; Chemical Industry Press: Beijing, 2010; pp 377−388.
(41) Khoso, S. A.; Hu, Y.; Lü, F.; Gao, Y.; Liu, R.; Sun, W. Xanthate interaction and flotation separation of H_2O_2-treated chalcopyrite and pyrite. *Trans. Nonferrous Met. Soc. China* **2019**, *29*, 2604−2614.

https://doi.org/10.1021/acsomega.3c03663
ACS Omega 2023, 8, 30474−30482

(42) Yao, W.; Li, M.; Zhang, M.; Cui, R.; Shi, J.; Ning, J. Decoupling the effects of solid and liquid phases in a Pb-water glass mixture on the selective flotation separation of scheelite from calcite. *Miner. Eng.* **2020**, *154*, 106423.
(43) Yao, W.; Li, M.; Zhang, M.; Cui, R.; Shi, J.; Ning, J. Effects of Pb^{2+} ions on the flotation behavior of scheelite, calcite, and fluorite in the presence of water glass. *Colloids Surf., A* **2022**, *632*, 127826.
(44) Jiang, X.; Zhang, W.; Fan, R.; Zhang, Z.; Chen, S.; Pooley, S.; Yang, L.; Gao, Z. Improved flotation of chalcopyrite from galena and pyrite by employing Cu-affinity phosphate collector. *Miner. Eng.* **2023**, *197*, 108064.
(45) Peng, W.; Liu, S.; Cao, Y.; Wang, W.; Lv, S.; Huang, Y. A novel approach for selective flotation separation of chalcopyrite and molybdenite-Electrocatalytic oxidation pretreatment and its mechanism. *Appl. Surf. Sci.* **2022**, *597*, 153753.
(46) Zhao, Q.; Yang, H.; Tong, L.; Jin, R.; Ma, P. Understanding the effect of grinding media on the adsorption mechanism of cyanide to chalcopyrite surface by ToF-SIMS, XPS, contact angle, zeta potential and flotation. *Colloids Surf., A* **2022**, *644*, 128799.
(47) NIST X-ray Photoelectron Spectroscopy Database, 2012. http://dx.doi.org/10.18434/T4T88K (accessed on 2023-05-20).

https://doi.org/10.1021/acsomega.3c03663
ACS Omega 2023, 8, 30474−30482